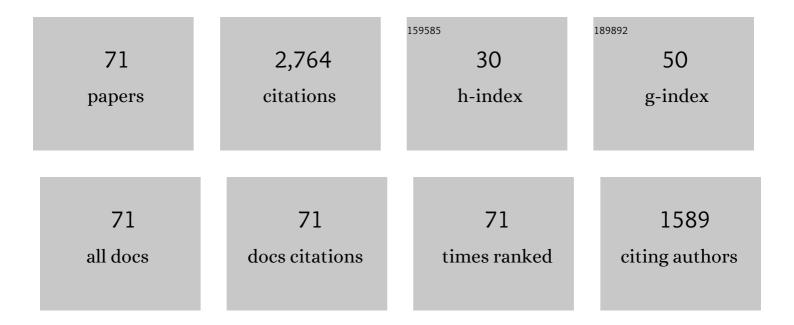
Guangdong Zhou

List of Publications by Year in descending order

Source: https://exaly.com/author-pdf/5183917/publications.pdf Version: 2024-02-01



#	Article	IF	CITATIONS
1	Coexistence of Negative Differential Resistance and Resistive Switching Memory at Room Temperature in TiO <i>_x</i> Modulated by Moisture. Advanced Electronic Materials, 2018, 4, 1700567.	5.1	147
2	A Unified Capacitive-Coupled Memristive Model for the Nonpinched Current–Voltage Hysteresis Loop. Nano Letters, 2019, 19, 6461-6465.	9.1	128
3	An organic nonvolatile resistive switching memory device fabricated with natural pectin from fruit peel. Organic Electronics, 2017, 42, 181-186.	2.6	119
4	Artificial and wearable albumen protein memristor arrays with integrated memory logic gate functionality. Materials Horizons, 2019, 6, 1877-1882.	12.2	116
5	Resistive switching memory integrated with amorphous carbon-based nanogenerators for self-powered device. Nano Energy, 2019, 63, 103793.	16.0	111
6	Biomemristors as the next generation bioelectronics. Nano Energy, 2020, 75, 104938.	16.0	110
7	Synaptic devices based neuromorphic computing applications in artificial intelligence. Materials Today Physics, 2021, 18, 100393.	6.0	110
8	Capacitive effect: An original of the resistive switching memory. Nano Energy, 2020, 68, 104386.	16.0	102
9	Negative Photoconductance Effect: An Extension Function of the TiO <i>_x</i> â€Based Memristor. Advanced Science, 2021, 8, 2003765.	11.2	94
10	Volatile and Nonvolatile Memristive Devices for Neuromorphic Computing. Advanced Electronic Materials, 2022, 8, .	5.1	94
11	Investigation of the behaviour of electronic resistive switching memory based on MoSe2-doped ultralong Se microwires. Applied Physics Letters, 2016, 109, .	3.3	86
12	ABO ₃ multiferroic perovskite materials for memristive memory and neuromorphic computing. Nanoscale Horizons, 2021, 6, 939-970.	8.0	79
13	Investigation of a submerging redox behavior in Fe2O3 solid electrolyte for resistive switching memory. Applied Physics Letters, 2019, 114, .	3.3	78
14	Coordinated Optical Matching of a Texture Interface Made from Demixing Blended Polymers for High-Performance Inverted Perovskite Solar Cells. ACS Nano, 2020, 14, 196-203.	14.6	64
15	A flexible nonvolatile resistive switching memory device based on ZnO film fabricated on a foldable PET substrate. Journal of Colloid and Interface Science, 2018, 520, 19-24.	9.4	59
16	Effect of Cu ions assisted conductive filament on resistive switching memory behaviors in ZnFe2O4-based devices. Journal of Alloys and Compounds, 2017, 694, 464-470.	5.5	52
17	Mechanism analysis of a flexible organic memristive memory with capacitance effect and negative differential resistance state. APL Materials, 2019, 7, .	5.1	51
18	Resistive switching behaviors and memory logic functions in single MnO _x nanorod modulated by moisture. Chemical Communications, 2019, 55, 9915-9918.	4.1	51

GUANGDONG ZHOU

#	Article	IF	CITATIONS
19	Metal ion formed conductive filaments by redox process induced nonvolatile resistive switching memories in MoS 2 film. Applied Surface Science, 2017, 426, 812-816.	6.1	50
20	Hydrogen-peroxide-modified egg albumen for transparent and flexible resistive switching memory. Nanotechnology, 2017, 28, 425202.	2.6	48
21	Mechanism for an enhanced resistive switching effect of bilayer NiO /TiO2 for resistive random access memory. Journal of Alloys and Compounds, 2017, 722, 753-759.	5.5	48
22	Nanorod Array of SnO ₂ Quantum Dot Interspersed Multiphase TiO ₂ Heterojunctions with Highly Photocatalytic Water Splitting and Self-Rechargeable Battery-Like Applications. ACS Applied Materials & Interfaces, 2019, 11, 2071-2081.	8.0	48
23	Evolution map of the memristor: from pure capacitive state to resistive switching state. Nanoscale, 2019, 11, 17222-17229.	5.6	45
24	Non-zero-crossing current-voltage hysteresis behavior induced by capacitive effects in bio-memristor. Journal of Colloid and Interface Science, 2020, 560, 565-571.	9.4	41
25	Refining the Negative Differential Resistance Effect in a TiO _{<i>x</i>} -Based Memristor. Journal of Physical Chemistry Letters, 2021, 12, 5377-5383.	4.6	41
26	Photoinduced triboelectric polarity reversal and enhancement of a new metal/semiconductor triboelectric nanogenerator. Nano Energy, 2019, 58, 331-337.	16.0	39
27	A high voltage direct current droplet-based electricity generator inspired by thunderbolts. Nano Energy, 2021, 90, 106567.	16.0	39
28	Improved Rate and Cycling Performances of Electrodes Based on BiFeO ₃ Nanoflakes by Compositing with Organic Pectin for Advanced Rechargeable Na-Ion Batteries. ACS Applied Nano Materials, 2018, 1, 1291-1299.	5.0	34
29	A larger nonvolatile bipolar resistive switching memory behaviour fabricated using eggshells. Current Applied Physics, 2017, 17, 235-239.	2.4	33
30	An excellent pH-controlled resistive switching memory device based on self-colored (C ₇ H ₇ O ₄ N) _n extracted from a lichen plant. Journal of Materials Chemistry C, 2019, 7, 7593-7600.	5.5	31
31	Highly Efficient Sn–Pb Perovskite Solar Cell and Highâ€Performance Allâ€Perovskite Fourâ€Terminal Tandem Solar Cell. Solar Rrl, 2020, 4, 1900396.	5.8	30
32	A Battery-Like Self-Selecting Biomemristor from Earth-Abundant Natural Biomaterials. ACS Applied Bio Materials, 2021, 4, 1976-1985.	4.6	30
33	Two-bit memory and quantized storage phenomenon in conventional MOS structures with double-stacked Pt-NCs in an HfAlO matrix. Physical Chemistry Chemical Physics, 2016, 18, 6509-6514.	2.8	26
34	Real-Time Acid Rain Sensor Based on a Triboelectric Nanogenerator Made of a PTFE–PDMS Composite Film. ACS Applied Electronic Materials, 2021, 3, 4162-4171.	4.3	22
35	An analogue memristor made of silk fibroin polymer. Journal of Materials Chemistry C, 2021, 9, 14583-14588.	5.5	22
36	Multi-factor-controlled ReRAM devices and their applications. Journal of Materials Chemistry C, 2022, 10, 8895-8921.	5.5	22

GUANGDONG ZHOU

#	Article	IF	CITATIONS
37	Memory characteristics and tunneling mechanism of Pt nano-crystals embedded in HfAlO films for nonvolatile flash memory devices. Current Applied Physics, 2015, 15, 279-284.	2.4	21
38	Band gap energies for white nanosheets/yellow nanoislands/purple nanorods of CeO ₂ . RSC Advances, 2016, 6, 59370-59374.	3.6	21
39	Resistance switching characteristics of core–shell γ-Fe2O3/Ni2O3 nanoparticles in HfSiO matrix. Journal of Alloys and Compounds, 2016, 678, 31-35.	5.5	20
40	A Weavable and Scalable Cotton‥arnâ€Based Battery Activated by Human Sweat for Textile Electronics. Advanced Science, 2022, 9, e2103822.	11.2	20
41	Current-voltage hysteresis of the composite MoS2-MoOâ‰ 9 nanobelts for data storage. Journal of Alloys and Compounds, 2016, 679, 47-53.	5.5	19
42	Effect of temperature on the magnetism and memristive memory behavior of MoSe 2 nanosheets. Materials Letters, 2017, 202, 13-16.	2.6	19
43	Self-woven monolayer polyionic mesh to achieve highly efficient and stable inverted perovskite solar cells. Chemical Engineering Journal, 2022, 428, 132074.	12.7	19
44	Applications of biomemristors in next generation wearable electronics. Nanoscale Horizons, 2022, 7, 822-848.	8.0	19
45	Passive Filters for Nonvolatile Storage Based on Capacitive-Coupled Memristive Effects in Nanolayered Organic–Inorganic Heterojunction Devices. ACS Applied Nano Materials, 2020, 3, 5045-5052.	5.0	18
46	Investigation of multi-photoconductance state induced by light-sensitive defect in TiO <i>x</i> -based memristor. Applied Physics Letters, 2022, 120, .	3.3	18
47	Bipolar resistive switching memory behaviors of the micro-size composite particles. Composite Structures, 2017, 166, 177-183.	5.8	17
48	A True Random Number Generator Based on Ionic Liquid Modulated Memristors. ACS Applied Electronic Materials, 2021, 3, 2380-2388.	4.3	17
49	Tunneling of photon-generated carrier in the interface barrier induced resistive switching memory behaviour. Journal of Colloid and Interface Science, 2019, 553, 682-687.	9.4	16
50	A novel retractable spring-like-electrode triboelectric nanogenerator with highly-effective energy harvesting and conversion for sensing road conditions. RSC Advances, 2017, 7, 50993-51000.	3.6	15
51	Self-Powered Memory Systems. , 2020, 2, 1669-1690.		15
52	TSSM: Three-State Switchable Memristor Model Based on Ag/TiOx Nanobelt/Ti Configuration. International Journal of Bifurcation and Chaos in Applied Sciences and Engineering, 2021, 31, 2130020.	1.7	15
53	A flexible piezoelectric-triboelectric hybrid nanogenerator in one structure with dual doping enhancement effects. Current Applied Physics, 2021, 32, 50-58.	2.4	15
54	Analog-to-digital and self-rectifying resistive switching behavior based on flower-like δ-MnO2. Applied Surface Science, 2022, 595, 153560.	6.1	15

#	Article	IF	CITATIONS
55	Enhancing the open circuit voltage of PEDOT:PSS-PC61BM based inverted planar mixed halide perovskite solar cells from 0.93 to 1.05 V by simply oxidizing PC61BM. Organic Electronics, 2018, 59, 260-265.	2.6	14
56	Memristor-Based Hierarchical Attention Network for Multimodal Affective Computing in Mental Health Monitoring. IEEE Consumer Electronics Magazine, 2023, 12, 94-106.	2.3	14
57	Pentacene as a hole transport material for high performance planar perovskite solar cells. Current Applied Physics, 2018, 18, 1095-1100.	2.4	13
58	Elimination of Charge Transport Layers in High-Performance Perovskite Solar Cells by Band Bending. ACS Applied Energy Materials, 2021, 4, 1294-1301.	5.1	13
59	The interface degradation of planar organic–inorganic perovskite solar cell traced by light beam induced current (LBIC). RSC Advances, 2017, 7, 42973-42978.	3.6	12
60	Multilevel resistive switching memory behaviors arising from ion diffusion and photoelectron transfer in α-Fe2O3 nano-island arrays. Physical Chemistry Chemical Physics, 2020, 22, 2743-2747.	2.8	11
61	Visible light-induced resistive switching behaviors in single MnO nanorod: Reversing between resistor and memristor. Journal of Alloys and Compounds, 2019, 802, 546-552.	5.5	10
62	Cobalt Phosphates Loaded into Iodine-Spaced Reduced Graphene Oxide Nanolayers for Electrochemical Measurement of Superoxide Generated by Cells. ACS Applied Nano Materials, 2021, 4, 3631-3638.	5.0	9
63	Reduction 93.7% time and power consumption using a memristor-based imprecise gradient update algorithm. Artificial Intelligence Review, 2022, 55, 657-677.	15.7	9
64	QuantBayes: Weight Optimization for Memristive Neural Networks via Quantization-Aware Bayesian Inference. IEEE Transactions on Circuits and Systems I: Regular Papers, 2021, 68, 4851-4861.	5.4	9
65	Mechanism analysis of switching direction transformation in an Er2O3 based RRAM device. Current Applied Physics, 2019, 19, 1421-1426.	2.4	7
66	Mechanism and Application of Capacitive-Coupled Memristive Behavior Based on a Biomaterial Developed Memristive Device. ACS Applied Electronic Materials, 2021, 3, 5537-5547.	4.3	7
67	Structure, Magnetism, and Electronic Properties of Inverse Heusler Alloy Ti2CoAl/MgO(100) Herterojuction: The Role of Interfaces. Applied Sciences (Switzerland), 2018, 8, 2336.	2.5	6
68	Memristive System Based Image Processing Technology: A Review and Perspective. Electronics (Switzerland), 2021, 10, 3176.	3.1	6
69	Real-time biomimetically monitoring superoxide anions released from transient transmembrane secretion to investigate the inhibition effect on Aspergillus flavus growth. Sensing and Bio-Sensing Research, 2020, 29, 100363.	4.2	3
70	First-principles study on the structure, magnetism, and electronic properties in inverse Heusler alloy Ti2FeAl/GaAs(100) heterojunction. Superlattices and Microstructures, 2019, 133, 106205.	3.1	2
71	The N, N-Dimethylformamide Annealing for Enhanced Performance of Perovskite Solar Cells Fabricated in Ambient Air. Nano, 2018, 13, 1850102.	1.0	0